Solubility Based Identification of Green Solvents for Small Molecule Organic Solar Cells

*Ignasi Burgués-Ceballos, Florian Machui, Jie Min, Tayebeh Ameri, Monika M. Voigt, Yuriy N. Luponosov, Sergei A. Ponomarenko, Paul D. Lacharmoise, Mariano Campoy-Quiles, and Christoph J. Brabec**

Replacing halogenated solvents in the processing of organic solar cells by green solvents is a required step before the commercialization of this technology. With this purpose, some attempts have been made, although a general method is yet to be developed. Here, the potential of the Hansen solubility parameters (HSP) analysis for the design of green ink formulations for solution-processed active layer in bulk heterojunction photovoltaic devices based on small molecules is demonstrated. The motivation of moving towards organic small molecules stems from their lower molecular weight and more definite structure which makes them more likely to be dissolved in a wider variety of organic solvents. In the first step, the HSP of selected active materials are determined, namely, the star-shaped D-π-A tris{4-[5″-(1,1-dicyanobut-1-en-2-yl)-2,2′-bithiophen-5-yl]phenyl}amine N(Ph-2T-DCN-Et)$_3$ small molecule and fullerene derivative [6,6]-phenyl-C_{71}-butyric acid methyl ester ($PC_{70}BM$). Secondly, computer simulations based on HSP allow the prediction of suitable green solvents for this specific material system. The most promising green solvents, according to the simulations, are then used to fabricate solar cell devices using pristine solvents and two solvents mixtures. These devices show power conversion efficiencies around 3.6%, which are comparable to those obtained with halogenated solvents. This good performance is a result of the sufficient solubility achieved after a successful prediction of good (green) solvents.

1. Introduction

The interest in organic photovoltaic (OPV) devices based on bulk-heterojunction structures continues to increase due to its potential to become a low-cost, light-weight alternative to conventional photovoltaic technologies. Given the possibility of solution processing, an important feature of organic semiconductors is their compatibility with large-scale printing and coating processes such as roll-to-roll.[1]

Halogenated solvents such as chlorobenzene or o-dichlorobenzene have been widely used in both polymer[2] and small molecule[3] solar cells due to their well known good solubility performance. However, the toxicity of these solvents as well as their high energy consuming synthesis makes them unfavorable in terms of sustainable development. Needless to say, their ban in mass production in industrial countries with strict environmental health and safety (EHS) legislation evidences the need for green formulations. When environmentally friendly solvents can be used, there is no need for expensive housings or expensive waste disposals. In this sense, some attempts have been made in the last few years to find non-hazardous solvents to process the active layer in OPVs.[4–10] For instance, the use of pristine o-xylene and 1,2,4-trimethylbenzene for processing the workhorse P3HT:PCBM system was reported,[4,5] although the resulting power conversion efficiencies (2.90% with o-xylene and 1.47% with 1,2,4-trimethylbenzene) were lower than the chlorinated counterpart. Moving another step forward, the mesitylene/acetophenone solvent blend reported by Park et al.[6] showed higher efficiency for the same material system (3.38%). On the other hand, less attention has been paid by the research community on the toxicity, costs and production energy related to the synthesis of organic semiconductors. Even so, recent works on the field give interesting perspectives on costs associated to the synthesis of the active materials,[11] their life cycle embodied energy[12] and alternative green chemistry reactions.[13] The goal of this work is, however, centered around the research of green solvents for the solution processing of the active layer.

I. Burgués-Ceballos, F. Machui, J. Min, Dr. T. Ameri, Prof. C. J. Brabec
Institute Materials for Electronics and Energy Technology (i-MEET)
University Erlangen-Nürnberg
Martensstrasse 7, 91058, Erlangen, Germany
E-mail: christoph.brabec@ww.uni-erlangen.de
I. Burgués-Ceballos, Dr. P. D. Lacharmoise
Cetemmsa Technological Centre
Av. Ernest Lluch 36, 08302, Mataró, Spain
I. Burgués-Ceballos, Dr. M. Campoy-Quiles
Institut de Ciència de Materials de Barcelona (ICMAB-CSIC), Esfera UAB, 08193, Bellaterra, Spain
Dr. M. M. Voigt, Prof. C. J. Brabec
Bavarian Center for Applied Energy Research (ZAE Bayern)
Haberstrasse 2a, 91058, Erlangen, Germany
Dr. Y. N. Luponosov, Prof. S. A. Ponomarenko
Enikolopov Institute of Synthetic Polymeric Materials of the Russian Academy of Sciences
Profsoyuznaya 70, Moscow, 117393, Russia
Prof. S. A. Ponomarenko
Lomonosov Moscow State University
Leninskie Gory, Moscow, 119991, Russia

DOI: 10.1002/adfm.201301509

Two major issues need to be taken into account in the design of ink formulations: 1) the solubility of the solute in the given solvent/s; and 2) the drying kinetics. Since the latter is connected to the vapor pressure, it is often controlled by modifying the deposition conditions such as speed and temperature. The solubility, however, is more difficult to control beyond the modest solubility increase obtained by heating the solution to higher temperatures.

Recently, several groups have studied the impact of the molecular solubility on the performance of both polymer[4,14–16] and small molecule[7] solution-processed solar cells. This growing interest in solubility has lead to the search of suitable tools for its study. One interesting tool is the Hansen solubility parameters (HSP) analysis, which has been demonstrated to provide relevant insights into different key aspects in OPVs such as the morphology of the bulk heterojunction layer,[17] finding suitable additives,[18] or new formulations that may enable to replace halogenated solvents.[4,6–8]

We have recently shown for a polymer:fullerene system that alternative green solvents can be identified by determining in the first place the solubility parameters for the materials under investigation and, in a second step, comparing the solubility parameters for the donor and acceptor materials with tabulated data for different solvents.[4] It would be particularly interesting to generalize our findings to other materials systems in order to advance a simple general rationale for the identification of green solvents and, in particular, those compatible with small molecule based OPV. In contrast to the low purity and wide molecular weight distribution of polymers,[19] organic small molecules offer some advantages such as well-defined molecular structure, higher purity and more definite molecular weight distribution without batch derived variations.[20] Furthermore, as a general rule lower molecular weight is related to higher solubility, besides the molecular moieties. As an example, the solubility of alcohols in water decreases as the molecular size of the alcohol molecule increases. Therefore, a strong motivation to move towards small molecules arises, since small molecules are more likely to be soluble in a wider variety of (green) solvents. Other aspects related to their synthesis like higher reproducibility, lower synthetic effort and thus potentially cheaper processing may also support this motivation.

The concept of solubility parameter was first introduced by Hildebrand and Scott,[21] who defined it as the square root of the energy of vaporization density and then extended by Hansen by separating this parameter into three contributions, known as Hansen solubility parameters (HSP). These are, namely, the (atomic) dispersive forces (δ_D), the (molecular) permanent dipole-permanent dipole (polar) interactions (δ_P), and the (molecular) hydrogen-bonding interactions (δ_H):

$$\delta^2 = \delta_D^2 + \delta_P^2 + \delta_H^2 \quad (1)$$

Plotting the HSP in a three dimensional "solubility" space, also known as Hansen space, allows us to define a solubility sphere wherein the solubility of the solute is above a given threshold. Within this space, the distance between two molecular species is inversely proportional to their mutual solubility. Therefore, in order to see how compatible different solvents might be with a given material, we should determine their corresponding HSPs and calculate how far they are from each other. Further description is given in the supplementary information.

The aim of the present work is to use the HSP analysis to find suitable non-halogenated solvents for two small molecules used as donor and acceptor materials in OPVs and correlate the predicted solubility behavior to the resulting photovoltaic performance. We use our recently developed binary solvent gradient method[4] for the determination of the HSP of a star-shaped small molecule and a fullerene derivative. The synthesis and photovoltaic properties of D-π-A star-shaped molecule tris{4-[5''-(1,1-dicyanobut-1-en-2-yl)-2,2'-bithiophen-5-yl]phenyl} amine N(Ph-2T-DCN-Et)$_3$ (**Figure 1**) were first reported in ref.[22] The small molecule was blended with [6,6]-phenyl-C_{71}-butyric acid methyl ester ($PC_{70}BM$) in chlorobenzene (CB) with the addition of 4-bromoanisole (BrAni) and used as the active layer in solar cells resulting in a 3.60% optimized power conversion efficiency (PCE). As it can be seen in Figure 1, the molecular structure of the star-shaped molecule consists in an aromatic core, three bithiophene bridging units and three polar ending groups. These different moieties may have dissimilar affinity to organic solvents, resulting in several chemical interactions. Thus, a wide variety of (non-chlorinated) solvents might be suitable to dissolve the molecule. Computer simulations allow us to determine compatible green solvents with these two molecules in terms of solubility. We fabricate OPVs using the predicted green solvents and obtain very good efficiencies, comparable to the halogenated counterparts.

2. Results and Discussion

2.1. Determination of HSP of N(Ph-2T-DCN-Et)$_3$ and $PC_{70}BM$ Using the Binary Solvent Gradient Method

We use the binary solvent gradient method to determine the HSP for the investigated materials. As already mentioned this method provides a precise determination of the HSP volume of a solute and enables the estimation of the Hansen surface with high accuracy.[4]

The first step consists in measuring the absolute solubility of the solutes in at least three different binary solvent gradients. The absolute solubility values of N(Ph-2T-DCN-Et)$_3$ and $PC_{70}BM$ in their corresponding series of solvent blends are presented in **Figure 2**. Exponential behaviors are expected with solubility increasing when going from the non-solvent rich solutions to the good solvent rich solutions.[4] This is in fact what is observed for the binary mixtures studied for $PC_{70}BM$, where similar trends are obtained for the 3 tested non-solvents. The most noticeable fact is the absolute solubility value of $PC_{70}BM$ in pristine chlorobenzene (207 mg mL^{-1}), which shows more than a threefold increase with respect to reported values for $PC_{60}BM$ (60 mg mL^{-1}).[4,14] As compared to the results reported for $PC_{60}BM$,[4] the trend with the 3 solvent blends is nearly comparable, being in both cases the binary CB/DMSO mixture the blend which gives higher solubilities.

The exponential tendency is also observed for the small molecule in CB/cyclohexane, CB/2-propanol and CB/acetone solvent blends, although different trends are observed. More surprisingly, in CB/propylene carbonate mixture (Figure 2a), higher

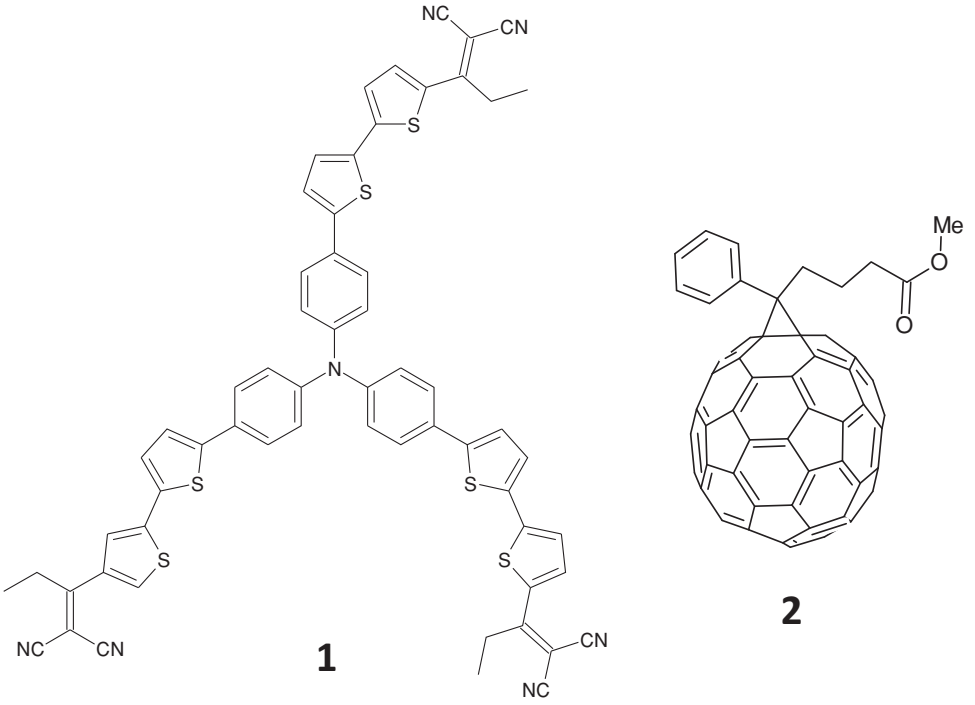

Figure 1. Molecular structures of 1) N(Ph-2T-DCN-Et)$_3$ and 2) $PC_{70}BM$.

solubility in comparison to pristine CB is obtained with 80% vol of CB. Although pristine propylene carbonate cannot be considered as good solvent for the material itself, this behavior when mixing with a good solvent such as chlorobenzene can be explained in terms of HSP reasoning, which in turn can explain the differences between the CB/2-propanol, CB/cyclohexane and CB/acetone mixtures. This will be discussed later in the text.

These data were introduced in the HSPiP software[23] database in order to predict the HSP for the materials under study. This prediction employed the standard fitting routine while the solubility space was assumed to be spherical. Following our previous work,[4] in order to investigate the predictions of the binary solvent gradient blend method for the HSP for both donor and acceptor materials, four solubility thresholds were chosen: 10 mg mL^{-1}, 5 mg mL^{-1}, 2 mg mL^{-1}, and 0.5 mg mL^{-1}.

As an example, the Hansen diagram for the solubility threshold of 10 mg mL^{-1} is shown in **Figure 3**. Every point represents a specific blend composition related to Figure 2. Blue circles correspond to solvent blend compositions that show solubility values above 10 mg mL^{-1} and thus are inside the green sphere, which represents the solubility volume of the solute. On the other hand, red squares represent the counterpart solvent blends with lower solubility. In the case of the star-shaped molecule higher accuracy of the volume of the sphere (i.e., R_0 radius) was obtained by introducing 4 axes instead of 3 in the HSP determination.

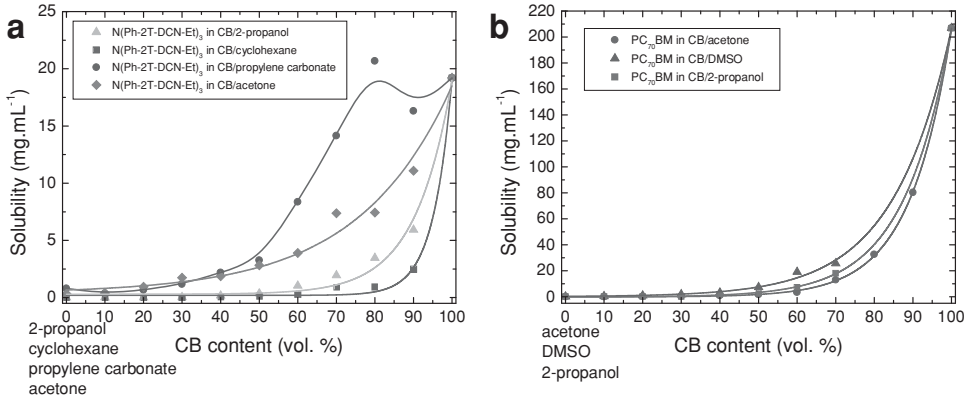

Figure 2. Solubility of a) N(Ph-2T-DCN-Et)$_3$ and b) $PC_{70}BM$ in solvent blends. Solid lines represent the exponential fit except for CB/propylene carbonate gradient in (a), where act as guide to the eye.

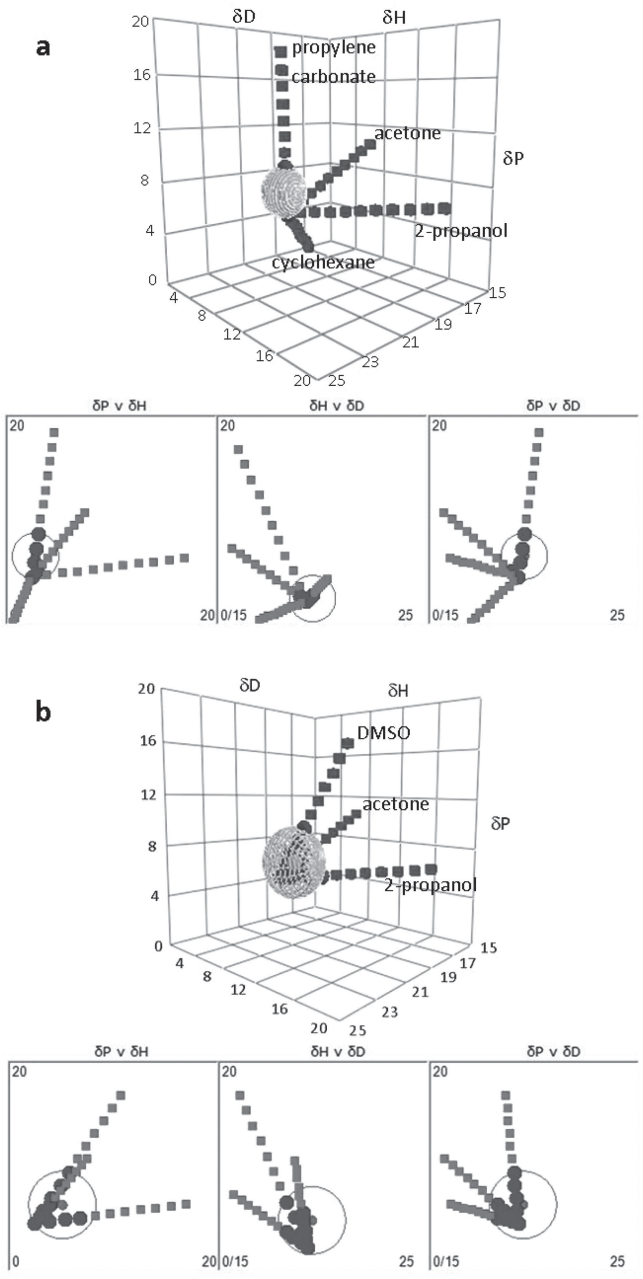

Figure 3. 3D and 2D HSP diagrams of a) N(Ph-2T-DCN-Et)$_3$ and b) $PC_{70}BM$ with solubility limit of 10 mg mL^{-1} (sphere). Circles correspond to solvents that are inside the sphere and squares to those external (all units of HSP are in MPa$^{1/2}$).

It can be seen in Figure 3 how the selected solvent gradients describe clear different directions in the Hansen space. The choice of solvents was done by taking their different preferential HSP contributions into account, which have an obvious relationship with their specific chemical structures. For instance, propylene carbonate and cyclohexane are high polar and non-polar solvents, respectively (preferential δ_P contribution), whereas the alcohol group in 2-propanol gives a higher hydrogen bonding (δ_H) contribution to this solvent.

Another important fact deduced from Figure 3 is that pristine chlorobenzene (origin of the 4 axes) is not located very close to the centre of the N(Ph-2T-DCN-Et)$_3$ solubility sphere. Although CB was chosen as "good solvent", it was of course not yet known how "good" it was (i.e., how close to the centre of the sphere it is). Moreover, some points in the CB/propylene carbonate gradient are closer than pristine CB to the centre of the sphere (i.e., with lower R_a). This explains the unexpected higher solubility values obtained at those points (Figure 2a).

The obtained HSP for both donor and acceptor materials are summarized in **Table 1**.

A high fitting accuracy was obtained in all cases and for both materials. Despite being molecules totally different in terms of molecular structure (see Figure 1), HSP for N(Ph-2T-DCN-Et)$_3$ and $PC_{70}BM$ do not differ very noticeably. More in detail, the disperse contribution is slightly higher for the fullerene derivative while the polar contribution (permanent dipole-permanent dipole interactions) is a bit higher for the small molecule. Higher differences are observed in the hydrogen bonding contribution, which is twice larger in the case of $PC_{70}BM$. Last, higher radii are obtained for $PC_{70}BM$, which indicate bigger solubility volume in the Hansen space.

The fact that both materials are close to each other in the Hansen space has a big impact in the research of suitable solvents for the N(Ph-2T-DCN-Et)$_3$:$PC_{70}BM$ blend. According to the theory related to HSP, those solvents which match the overlapping space defined by the spheres of the two materials would be ideal in terms of solubility (see **Figure 4**).

2.2. Finding Suitable Green Solvents

A series of 50 non-halogenated solvents was introduced in the HSPiP software and the HSP of N(Ph-2T-DCN-Et)$_3$ and $PC_{70}BM$ with the solubility limit set at 10 mg mL^{-1} were introduced as the target. A selection of 8 solvents is shown in Figure 4 and the values are summarized in **Table 2**.

As it can be seen in Figure 4, this first approximation reveals the potential of benzaldehyde for its use as a pristine solvent, since it fits within the space defined by both N(Ph-2T-DCN-Et)$_3$ and $PC_{70}BM$ spheres. The later determination of real absolute solubility of the small molecule in benzaldehyde revealed the surprisingly high value of 51.7 mg mL^{-1}. It is important to note that benzaldehyde is closest to $PC_{70}BM$ in the Hansen space, which indicates even higher solubility affinity as compared to N(Ph-2T-DCN-Et)$_3$. This can also be seen in Table 2 comparing the solubility distances (R_a, this is the distance in the solubility space between the centre of two spheres; see Supporting Information). Reassuringly, the solubility of $PC_{70}BM$ in benzaldehyde was found to be higher than 150 mg mL^{-1}. However, when comparing benzaldehyde and chlorobenzene, a different correlation is observed between the solubility distance to the small molecule (3.2 MPa s and 2.1 MPa s, respectively) and its real solubility in each solvent (51.7 mg mL^{-1} and 19.2 mg mL^{-1}, respectively). With a higher solubility in benzaldehyde, a lower distance would be expected (i.e., higher solubility affinity). Further work is being carried out to investigate if these discrepancies are derived from the assumption of a spherical shape

Table 1. Hansen solubility parameters for N(Ph-2T-DCN-Et)$_3$ and $PC_{70}BM$. The last two columns indicate the total number of solvent (blend) systems among the different gradients that showed solubilities above (below) the corresponding threshold and thus are inside (outside) the sphere. The fitting resulted in 0 wrong in and 0 wrong out points.

Solute	Solubility limit [mg mL^{-1}]	δ_D [MPa$^{1/2}$]	δ_P [MPa$^{1/2}$]	δ_H [MPa$^{1/2}$]	δ_{tot} [MPa$^{1/2}$]	R_0 [MPa$^{1/2}$]	In	Out
N(Ph-2T-DCN-Et)$_3$	10	19.20	6.33	2.28	20.35	2.1	5	36
	5	19.23	7.01	2.57	20.63	2.9	9	32
	2	19.05	8.19	2.74	20.91	4.5	15	26
	0.5	19.09	8.96	3.47	21.37	6.5	24	17
$PC_{70}BM$	10	19.15	6.07	4.61	20.61	3.2	11	20
	5	19.68	6.26	5.93	21.48	4.6	13	18
	2	19.82	6.60	6.82	21.98	5.6	16	15
	0.5	19.85	7.87	7.53	22.64	6.8	21	10

(instead of ellipsoidal) in this simplified method. Although the latter is yet not fully understood, the high solubility in benzaldehyde of N(Ph-2T-DCN-Et)$_3$ as well as the quite similar HSP of this solvent in comparison to good solvents such as o-dichlorobenzene (DCB) and chlorobenzene suggest that benzaldehyde may be a promising candidate to replace these halogenated solvents, which are widely used in the solution processing of semiconductors. A solid argument for the latter is given by the low R_a values between benzaldehyde and these two chlorinated solvents (2.32 MPa$^{1/2}$ and 4.60 MPa$^{1/2}$ for DCB and CB, respectively).

The second step involved the study of mixtures of 2 non-halogenated solvents. The goal is to get closer to the junction in the Hansen space (considering it as a non-pondered average of the HSP; see experimental section). To achieve this objective one has to think about 2 solvents located at different positions in the Hansen space in a way that the resulting line that connects the two points crosses the N(Ph-2T-DCN-Et)$_3$:$PC_{70}BM$ junction space as close as possible to its centre. This resulting line corresponds to the gradient of composition between these 2 solvents (see Supporting Information, Figure SI2). Apart from this, it is also important to take other properties into account such as the miscibility between each other and their boiling point. The latter has a high impact on the drying kinetics of the wet film, which in turn may have a strong influence on the morphology of the active layer.

The simulation performed with the HSPiP software revealed the potentiality of the solvent mixture comprised by benzaldehyde and mesitylene (1,3,5-trimethylbenzene). Figure SI2 (Supporting Information) shows the location of the 2 solvents in the Hansen space as well as some points in the gradient of the solvent composition. It is therein observed how the linking line between the two solvents gets closest to the junction at some point between the two solvents. This means that, according to Hansen theory, at that solvent composition the solubility of both materials will be higher. An illustrative way to represent

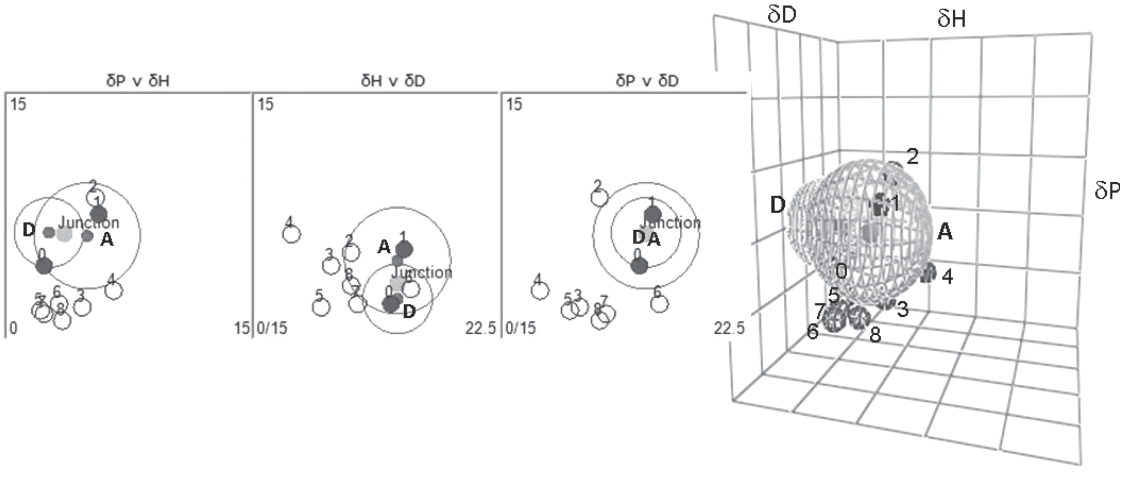

Figure 4. 2D and 3D plots of the distribution in Hansen space at 25 °C of several non-halogenated solvents (small circles) overlapped with the N(Ph-2T-DCN-Et)$_3$(D):$PC_{70}BM$(A) junction. Benzaldehyde (1) is the most suitable solvent for the blend, as it fits within the junction (shown as a filled circle in the software as well as reference CB, named as 0). The rest of solvents (empty small circles) are 2) cyclohexanone, 3) d-limonene, 4) oleic acid, 5) β-pinene, 6) 1,2,3,4-tetrahydronaphthalene, 7) toluene, and 8) o-xylene.

Table 2. Hansen solubility parameters of a selection of solvents. The absolute distance to HSP of N(Ph-2T-DCN-Et)$_3$, $PC_{70}BM$, and the junction is also shown. Further description available in the Supporting Information.

Solvent	δ_D [MPa$^{1/2}$]	δ_P [MPa$^{1/2}$]	δ_H [MPa$^{1/2}$]	R_a [MPa$^{1/2}$]		
				to N(Ph-2T-DCN-Et)$_3$[a)]	to $PC_{70}BM$[a)]	to junction[a)]
Halogenated						
chlorobenzene	19.0	4.3	2.0	2.1	3.2	2.7
o-dichlorobenzene	19.2	6.3	3.3	1.0	1.3	1.1
chloroform	17.8	3.1	5.7	5.5	4.3	4.7
p-bromoanisole	19.8	7.7	7.0	5.1	3.1	4.5
Non-halogenated						
toluene	18.0	1.4	2.0	5.5	5.9	5.5
o-xylene	17.8	1.0	3.1	6.1	6.0	5.9
tetrahydronaphthalene	19.6	2.0	2.9	4.5	4.5	5.0
mesitylene	18.0	0.6	0.6	6.4	7.2	6.7
cyclohexane	16.8	0.0	0.2	8.2	8.9	8.2
dimethyl sulfoxide	18.4	16.4	10.2	12.9	11.8	12.1
d-Limonene	17.2	1.8	4.3	6.1	5.9	5.8
β-pinene	16.9	1.6	1.8	6.6	6.9	6.6
Green solvents[b)]						
acetone	15.5	10.4	7.0	9.7	8.9	8.4
2-propanol	15.8	6.1	16.4	15.7	13.6	14.4
benzaldehyde	19.4	7.4	5.3	3.2	1.5	2.7
cyclohexanone	17.8	8.4	5.1	4.5	3.7	3.2
oleic acid	16.0	2.8	6.2	8.3	7.4	7.3
propylene carbonate	20.0	18.0	4.1	11.9	12.0	11.7

[a)]Calculated with the HSP obtained with the 10 mg mL^{-1} threshold; [b)]Not containing risk phrases R50/59, relative to harmfulness to environment (EU Dangerous Substances Directive (67/548/EEC)).

this is shown in **Figure 5**, where the solubility distance R_a is plotted as a function of the solvent composition.

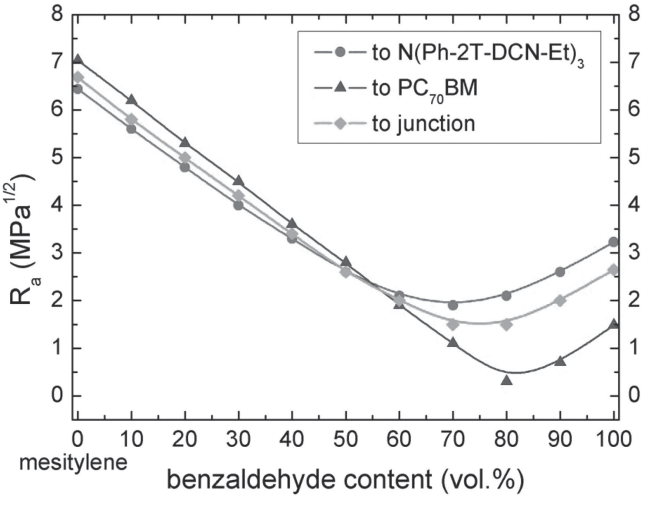

Figure 5. Absolute distance in Hansen space (R_a) as a function of benzaldehyde content in the benzaldehyde:mesitylene solvent mixture.

In accordance to this, a minimum R_a distance to both N(Ph-2T-DCN-Et)$_3$ and $PC_{70}BM$ as well as to the junction between them is seen in Figure 5 and with a 70–80% of benzaldehyde content.

2.3. OPV Fabrication with Green Formulations

In order to study the relationship between solubility and photovoltaic performance, small molecule OPV devices were prepared using pristine benzaldehyde or benzaldehyde:mesitylene (80:20) for the processing of the active layer. Reference devices were fabricated with chlorobenzene and mixtures of chlorobenzene with 2% of 4-bromoanisole additive, as described elsewhere.[22] The optimal doctor blading temperature for both benzaldehyde and benzaldehyde:mesitylene blend systems was set to 80 °C in order to guarantee an efficient drying.

The statistic spreading of the main performance parameters extracted from at least 15 solar cells for each solvent system are depicted in **Figure 6**. Reassuringly, the green solvent formulations result in a similar good performance as the chlorinated solvents, with practically negligible differences in all performance parameters. There might be a tendency

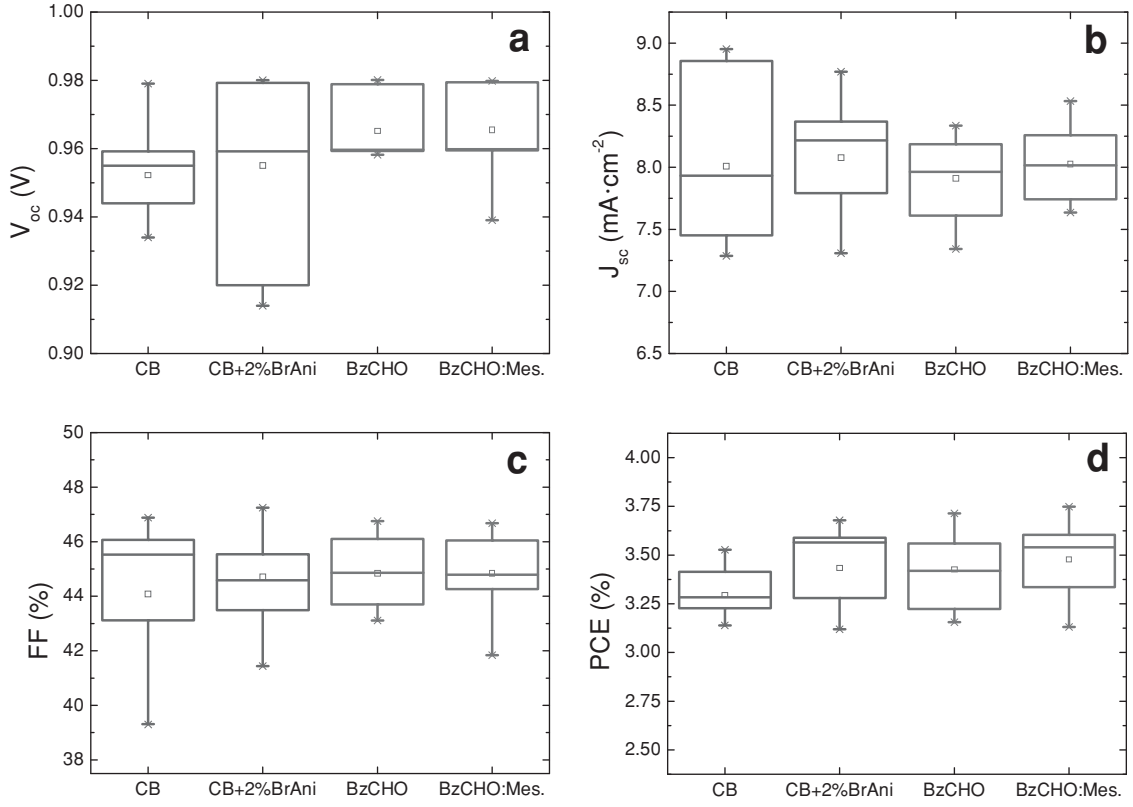

Figure 6. OPV performance parameters of devices based on chlorobenzene (CB), chlorobenzene with 2% of p-bromoanisole (CB+2% BrAni), benzaldehyde (BzCHO), and benzaldehyde:mestiylene (80:20) system (BzCHO:Mes.).

for improvement in PCE but it is not statistically significant. These comparable performances obtained with green solvents and halogenated formulations correlates with the theoretical solubility analysis previously described. Thus, the applicability of the Hansen theory in the design of green formulations is proved. Moreover, it is demonstrated that halogenated solvents can be successfully replaced without losing efficiency by properly studying the solubility characteristics of the materials and adjusting the drying conditions.

The resulting *J–V* curves from the best performing devices for each solvent system are plotted in **Figure 7**, and the corresponding parameters are summarized in **Table 3**. As far as we know, these are the best PCE values obtained via green solvents processing reported up to now.

Pristine benzaldehyde shows already a high solubility for both components, offering the possibility to reach similar device performance compared to halogenated solvent systems. By introducing a second solvent, mesitylene, with the simulated optimum blend composition, the PCE only improves slightly. The effect of the additional increase in solubility seems not to have a major effect in device performance in this case. In other words, our experiments suggest that there is a minimum solubility required

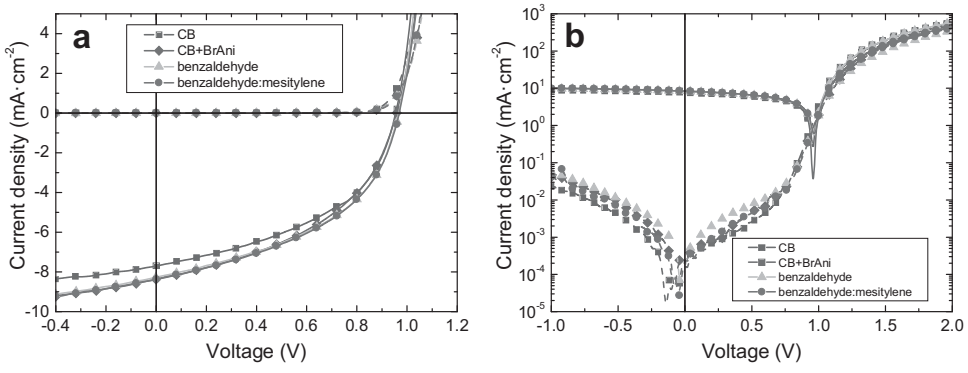

Figure 7. *J–V* curves of best performing devices based on chlorobenzene (CB), chlorobenzene with 2% of p-bromoanisole, benzaldehyde, and benzaldehyde:mesitylene (80:20) under AM 1.5G 100 mW cm^{-2} illumination (solid lines) and in dark conditions (dashed lines).

Table 3. OPV performance parameters of best performing devices based on different solvent systems.

Solvent system	V_{oc} [V]	J_{sc}[a)] [mA cm^{-2}]	J_{sc}[b)] [mA cm^{-2}]	FF [%]	PCE[a)] [%]	PCE[b)] [%]
chlorobenzene	0.96	7.71	7.56	46.11	3.41	3.34
chlorobenzene + 2% BrAni	0.96	8.32	7.95	45.22	3.61	3.45
benzaldehyde	0.96	8.27	8.06	46.75	3.71	3.62
benzaldehyde:mesitylene 80:20	0.96	8.37	8.35	46.68	3.75	3.74

[a)]Measured under AM1.5G 100 mW cm^{-2} illumination; [b)]Calculated from EQE spectra.

for the ink to be processable and lead to good performance, while further increases in solubility may not be expected to result in major benefits. Therefore, any additional mixing that keeps the solubility above the minimum can be employed to assist the drying kinetics of the specific deposition technique employed. However, under a strict environmental point of view, pristine benzaldehyde is greener than the mixture with mesitylene.

Nevertheless, the shape of the *J–V* curves (Figure 7) and the low fill factor may suggest that there is still room for improvement. Other factors such as morphology of the bulk heterojunction may limit the device performance. Atomic force microscopy images (Figure SI3, Supporting Information) indicate that the surface topology of the films fabricated with the four solvent systems (CB, CB+2%BrAni, benzaldehyde, and benzaldehyde:mesitylene) are very similar and consist of a fine mixing of the two components coupled to a low surface roughness (RMS < 1 nm in all cases). The almost overlapping absorption and external quantum efficiency (Supporting Information, Figure SI4) of devices fabricated with the different solvents suggest that an approximately comparable morphology is maintained throughout the depth of the film.

3. Conclusions

The binary solvent gradient method has been used to determine the Hansen solubility parameters of two different materials: the small molecule, star-shaped N(Ph-2T-DCN-Et)$_3$ and the fullerene derivative $PC_{70}BM$. The HSPs of both materials have then been used to predict suitable green formulations in terms of solubility for the solution processing of active layers. We first have focused on pristine solvents and have found benzaldehyde to be the most suitable solvent. Then, we have developed inks that included mixtures of two solvents (benzaldehyde:mesitylene (80:20)) in order to obtain a system with the closest solubility to the junction between the donor and acceptor solubility spheres (according to the Ra distance in the Hansen space). Finally, solar cells have been fabricated using these green formulations, resulting in similar power conversion efficiencies with both benzaldehyde (3.62%) and benzaldehyde:mesitylene mixture (3.74%) comparable to halogenated solvent systems (3.45%).

4. Experimental Section

The binary solvent gradient method was applied to determine the HSP values of the small molecules N(Ph-2T-DCN-Et)$_3$ and $PC_{70}BM$. First, three (for $PC_{70}BM$) or four (for N(Ph-2T-DCN-Et)$_3$) series of solvent mixtures consisting of blends of a non-solvent and a good solvent (chlorobenzene (CB) in both cases) were prepared for each material. Each series consists of a CB fraction X/(X+Y) and a non-solvent fraction Y/(X+Y), being X+Y equal to 100%. 2-propanol, cyclohexane, acetone and propylene carbonate were used as non-solvents for N(Ph-2T-DCN-Et)$_3$ while 2-propanol, acetone and dimethyl sulfoxide (DMSO) were the counterpart for $PC_{70}BM$. N(Ph-2T-DCN-Et)$_3$ (Heraeus) and $PC_{70}BM$ (technical grade from Solenne BV) were used as received. All the solvents were used as received from commercial chemical suppliers (Sigma-Aldrich). The series of solvent mixtures chosen for N(Ph-2T-DCN-Et)$_3$ describe 4 different directions within the Hansen space, with one dominant coordinate for each one, that is, the dispersive, the polar or the hydrogen bonding contribution. We used four rather than three solvent mixtures in order to improve accuracy in the determination of the HSP for this molecule. For the $PC_{70}BM$, the same 3 non-solvents were used as those for $PC_{60}BM$ in our previous work[4] in order to better compare the differences in solubility between both materials.

Determination of absolute solubility was done by preparing saturated solutions of the materials followed by stirring for at least twelve hours at room temperature and later centrifugation at 15 000 rpm for ten minutes. The centrifuged solutions were subsequently diluted to achieve an optical density suitable for absorption measurements. The absolute solubility for each solution was calculated by comparing its optical density to standard curves with known concentrations. Absorption profiles were recorded with a Perkin Elmer Lambda-950 absorption spectrometer from 350 to 700 nm. The measurements were performed at 25 °C.

For the determination of the Hansen Solubility Parameters the experimental solubility data were introduced in the HSPiP software developed by Abbott, Hansen, and Yamamoto.[23] As it is defined in the HSP prediction method,[24] a score of 1 is given to the points that show solubility values above the chosen solubility limit and a score of 0 to those points with lower solubility. This scoring is used by the software to predict the HSP as well as the radii of the sphere through a standard fitting routine. Four solubility thresholds were chosen to investigate the predictions of the binary solvent gradient blend method: 10 mg mL^{-1}, 5 mg mL^{-1}, 2 mg mL^{-1}, and 0.5 mg mL^{-1}.

Potentially suitable solvents for the N(Ph-2T-DCN-Et)$_3$:$PC_{70}BM$ junction were estimated by introducing a selection of 50 non-halogenated solvents into the HSPiP software. The determined HSP values for the two materials were then set as the target junction. The first estimation was performed at room temperature. All HSP values were later corrected for the different working temperatures. It is important to note that the target junction was considered as a non-pondered average of the HSP of the N(Ph-2T-DCN-Et)$_3$: $PC_{70}BM$ blend, regardless the donor to acceptor weight ratio used in the fabrication of the devices, as the main goal is to find suitable solvents for both pristine materials.

For the preparation of solar cells, laser-patterned ITO-coated glasses[25] were cleaned by successive steps using an ultrasonic bath in acetone and 2-propanol for 15 min each. A solution of poly(3,4-ethylenedioxythiophene):poly(styrenesulfonate) (PEDOT:PSS; Clevios P VP Al4083 from Heraeus) previously diluted in 2-propanol (1:3 volume ratio) was doctor bladed on top of the ITO surface at 50 °C with a blade speed of 10 mm s^{-1}, 60 µL of liquid volume and 400 µm of gap between

blade and substrate. An intermediate annealing step (5 min at 140 °C) was performed before doctor blading another PEDOT:PSS layer, with the same coating parameters. This double layer which helped to obtain a homogeneous blocking layer was again annealed for 15 min at 140 °C. The active layer was deposited by doctor blading a 2 wt% blend solution of N(Ph-2T-DCN-Et)$_3$ and $PC_{70}BM$ (1:2 wt ratio) in the solvent system. The 12 mm s-1 of blade speed, 60 µL of solution and 400 µm of gap resulted in a thickness of 80–90 nm for the active layer. The temperature of the doctor blade equipment stage was adjusted for each solvent system according to their different vapor pressures in order to achieve similar drying times (<5 s). Solutions based on chlorobenzene with 0% and 2% of BrAni additive were coated at 65 °C whereas those based on benzaldehyde and benzaldehyde:mesitylene (80:20) were coated at 80 °C. These two non-halogenated solvents were chosen according to the results of the HSP anaylsis, as it is discussed in the main text. Then, the samples were transferred into a nitrogen-filled glovebox where Ca (15 nm)/Ag (85 nm) electrodes were thermally evaporated at 3×10^{-6} mbar through a shadow mask, defining an active area of 10.4 mm^2. Finally, the devices were encapsulated with a glass cap using an ultraviolet curing epoxy resin (ELC 2500). The 2.5 min exposure to the UV radiation was performed from the Ag metal side to avoid photodegradation of the organic layers across the active region.

Current–voltage characteristics of the solar cells were measured under AM 1.5G irradiation on an OrielSol 1A Solar simulator (100 mW cm^{-2}). The external quantum efficiency (EQE) was determined using a Cary-5000 Spectrometer coupled with a Lock-in integrator (frequency of 30.0 Hz and 500 ms of integration time).

AFM measurements were performed with an Agilent 5100 equipment in tapping mode (5 µm × 5 µm of scan area).

Supporting Information

Supporting Information is available from the Wiley Online Library or from the author.

Acknowledgements

I.B.-C. and F.M. contributed equally to this work. The authors want to thank Dr. Andreas Elschner and Dr. Wilfried Lovenich from Heraeus Precious Metals GmbH & Co. KG, for supplying the D-π-A molecule as well as the Universitat Autònoma de Barcelona (UAB) for the support given through the Chemistry PhD program. This work was financially supported by the Spanish Ministry of Science and Innovation through projects MAT2009–10642 and PLE2009–0086. The authors also gratefully acknowledge the support of the European Commission as part of the seventh framework programme (ICT) collaborative project ROTROT (grant no. 288565), the Synthetic Carbon Allotropes (project no. SFB953) and the Cluster of Excellence "Engineering of Advanced Materials" at the University of Erlangen-Nuremberg which is funded by the German Research Foundation (DFG) within the framework of its "Excellence Initiative".

Received: May 2, 2013
Revised: August 28, 2013
Published online: November 4, 2013

[1] H. Hoppe, N. S. Sariciftci, *J. Mater. Res.* **2007**, *19*, 1924–1945.
[2] C. J. Brabec, S. Gowrisanker, J. J. M. Halls, D. Laird, S. Jia, S. P. Williams, *Adv. Mater.* **2010**, *22*, 3839–3856.
[3] B. Walker, C. Kim, T.-Q. Nguyen, *Chem. Mater.* **2010**, *23*, 470–482.
[4] F. Machui, S. Langner, X. Zhu, S. Abbott, C. J. Brabec, *Sol. Energy Mater. Sol. Cells* **2012**, *100*, 138–146.
[5] K. Tada, *Sol. Energy Mater. Sol. Cells* **2013**, *108*, 82–86.
[6] C.-D. Park, T. A. Fleetham, J. Li, B. D. Vogt, *Org. Electron.* **2011**, *12*, 1465–1470.
[7] B. Walker, A. Tamayo, D. T. Duong, X.-D. Dang, C. Kim, J. Granstrom, T.-Q. Nguyen, *Adv. Energy Mater.* **2011**, *1*, 221–229.
[8] F. Machui, S. Abbott, D. Waller, M. Koppe, C. J. Brabec, *Macromol. Chem. Phys.* **2011**, *212*, 2159–2165.
[9] A. Lange, W. Schindler, M. Wegener, K. Fostiropoulos, S. Janietz, *Sol. Energy Mater. Sol. Cells* **2013**, *109*, 104–110.
[10] K.-S. Chen, H.-L. Yip, C. W. Schlenker, D. S. Ginger, A. K.-Y. Jen, *Org. Electron.* **2012**, *13*, 2870–2878.
[11] T. P. Osedach, T. L. Andrew, V. Bulovic, *Energy Environ. Sci.* **2013**, *6*, 711–718.
[12] A. Anctil, C. W. Babbitt, R. P. Raffaelle, B. J. Landi, *Prog. Photovoltaics: Res. Appl.* **2012**.
[13] D. J. Burke, D. J. Lipomi, *Energy Environ. Sci.* **2013**, *6*, 2053.
[14] P. A. Troshin, H. Hoppe, J. Renz, M. Egginger, J. Y. Mayorova, A. E. Goryachev, A. S. Peregudov, R. N. Lyubovskaya, G. Gobsch, N. S. Sariciftci, V. F. Razumov, *Adv. Funct. Mater.* **2009**, *19*, 779–788.
[15] S. Nilsson, A. Bernasik, A. Budkowski, E. Moons, *Macromolecules* **2007**, *40*, 8291–8301.
[16] J.-H. Kim, J. H. Park, J. H. Lee, J. S. Kim, M. Sim, C. Shim, K. Cho, *J. Mater. Chem.* **2010**, *20*, 7398–7405.
[17] D. T. Duong, B. Walker, J. Lin, C. Kim, J. Love, B. Purushothaman, J. E. Anthony, T.-Q. Nguyen, *J. Polym. Sci. B: Polym. Phys.* **2012**, *50*, 1405–1413.
[18] K. R. Graham, P. M. Wieruszewski, R. Stalder, M. J. Hartel, J. Mei, F. So, J. R. Reynolds, *Adv. Funct. Mater.* **2012**, *22*, 4801–4813.
[19] M. Koppe, C. J. Brabec, S. Heiml, A. Schausberger, W. Duffy, M. Heeney, I. McCulloch, *Macromolecules* **2009**, *42*, 4661–4666.
[20] Y. Lin, X. Zhan, *Chem. Soc. Rev.* **2012**, *41*, 4245–4272.
[21] J. H. Hildebrand, R. L. Scott, *J. Chem. Phys.* **1952**, *20*, 1520–1521.
[22] J. Min, Y. N. Luponosov, T. Ameri, A. Elschner, S. M. Peregudova, D. Baran, T. Heumüller, N. Li, F. Machui, S. Ponomarenko, C. J. Brabec, *Org. Electron.* **2013**, *14*, 219–229.
[23] S. Abbott, C. M. Hansen, H. Yamamoto, Hansen Solubility Parameters in Practice, (software) Version 3.1.17, 2008–2011, www.hansen-solubility. com (accessed: August **2011**).
[24] C. M. Hansen, *Hansen Solubility Parameters – A User's Handbook*, 2nd ed., CRC Press, Boca Raton, FL. USA, **2007**, Ch. 1.
[25] P. Kubis, N. Li, T. Stubhan, F. Machui, G. J. Matt, M. M. Voigt, C. J. Brabec, *Prog. Photovoltaics Res. Appl.*, unpublished.